ELSEVIER

Hearing Research 127 (1999) 41–54

HEARING RESEARCH

Adjustable frequency selectivity of auditory forebrain neurons recorded in a freely moving songbird via radiotelemetry

Andreas Nieder [1], Georg M. Klump *

Institut für Zoologie, Technische Universität München, Lichtenbergstr. 4, 85747 Garching, Germany

Received 22 April 1998; received in revised form 10 September 1998; accepted 21 September 1998

Abstract

One of the hearing system's basic properties that determines the detection of signals is its frequency selectivity. In the natural environment, a songbird may achieve an improved detection ability if the neuronal filters of its auditory system could be sharpened to adapt to the spectrum of the background noise. To address this issue, we studied 35 multi-unit clusters in the input layer of the primary auditory forebrain of nine European starlings (*Sturnus vulgaris*). Microelectrodes were chronically implanted in this songbird's cortex analogue and the neuronal activity was transmitted from unrestrained birds via a miniature FM transmitter. Frequency tuning curves (FTCs) and inhibitory sidebands were determined by presenting a matrix of frequency-level combinations of pure tones. From each FTC, the characteristic frequency (CF) and several parameters describing the neurons' filter characteristics were derived and compared to the same recording site's filter function while simultaneously stimulating with a continuous CF tone 20 dB above the response threshold. Our results show a significant improvement of frequency selectivity during two-tone stimulation, indicating that spectral filtering in the starling's auditory forebrain depends on the acoustic background in which a signal is presented. Moreover, frequency selectivity was found to be a function of the time over which the stimulus persisted, since FTCs were much sharper and inhibitory sidebands were largely expanded several milliseconds after response onset. Neuronal filter bandwidths during two-tone stimulation in the auditory forebrain are in good agreement with psychoacoustically measured critical bandwidths in the same species. Radiotelemetry proved to be a powerful tool in studying neuronal activity in freely behaving birds.

Key words: Bird; Starling; Telemetry; Auditory forebrain; Field L; Frequency tuning; Two-tone interaction; Masking

1. Introduction

In the natural environment, acoustic signals have to be detected in a ubiquitous noisy background (for a review see Klump, 1996). The masking and distortion of acoustic signals by noise poses a severe problem for human speech perception and communication in birds as well. Songbirds – like the European starling (*Sturnus vulgaris*) – with their elaborate vocal repertoire are excellent subjects for studying how signals are perceived in a noisy world.

Frequency selectivity is one of the hearing system's basic properties that determine the detection of signals. According to the power-spectrum model of perception of Fletcher (1940), spectral filtering is accomplished by a bank of overlapping band-pass filters, each with its own center frequency. Sounds are most effective in masking a signal if their spectral components lie within the filter's bandwidth. The smaller the bandwidth of an auditory filter, the less the spectral energy of a masking noise falling within the filter's range and the better signal detection becomes. Recently, psychoacoustic data on spectral filtering have been reported for the starling (Langemann et al., 1995; Klump and Langemann,

* Corresponding author.
Tel.: +49 (89) 289-13668; Fax: +49 (89) 289-13674;
E-mail: gklump@star1.zoo.chemie.tu-muenchen.de

[1] Present address: Lehrstuhl für Zoologie/Tierphysiologie, Institut für Biologie II, RWTH Aachen, Kopernikusstr. 16, 52074 Aachen, Germany.

0378-5955/99/$ – see front matter
PII: S0378-5955(98)00179-8

1995). We therefore propose this bird species as a model to study the neuronal basis of spectral analysis.

Comparing perceptual auditory filters and their putative neuronal analogues, the frequency tuning curves (FTCs), the frequency selectivity at the level of auditory nerve fibers in mammals and the starling in general correlates well with psychophysical data describing the bandwidth of auditory filters (Pickles, 1979; Evans et al., 1992; Buus et al., 1995; Langemann et al., 1995). However, some observations from behavioral studies (e.g., the level independence of the signal-to-noise ratio needed for detection of a signal) are difficult to explain on the basis of the filter characteristics of auditory nerve fibers alone (e.g., see review by Ehret, 1988); additional shaping and sharpening of FTCs is required in more central parts of the auditory pathway. In some mammals, it has been observed that FTCs become sharper at higher levels of the auditory pathway (e.g., Katsuki et al., 1958; Suga and Tsuzuki, 1985). Moreover, level-independent frequency tuning during narrow-band masking was found both in the anesthetized cat's inferior colliculus (Ehret and Merzenich, 1985, 1988) and in the cat auditory cortex (Ehret, 1995; Ehret and Schreiner, 1997). This increase of frequency selectivity of neural filters along the auditory pathway may improve the individual's detection ability.

In this study, we present evidence that the filter characteristics of the starling's auditory forebrain neurons change dynamically in two ways. Firstly, the spectral filter characteristics of the tuning curves depended on the acoustic background in which a signal was presented. Secondly, the spectral filter characteristics of the tuning curves were found to be a function of the time over which the stimulus persisted. Furthermore, we demonstrate that data on auditory processing in a bird can be collected over an extended time period without restraint of the animal by using radiotelemetric transmission of neuronal activity.

2. Materials and methods

2.1. Fabrication of microelectrodes

The electrodes were prepared from polyimide-insulated nickel-chrome resistance wires ('Isaohm'; 75% Ni, 20% Cr, 4% Al) obtained from Isabellenhütte Dillenburg, Germany. Wires with core diameters of 17 μm were sharpened at the tip similar to the procedure described by Jacob and Krüger (1991). The wire insulation was burned off at both ends and the exposed tip of one end was etched electro-chemically in a 1:500 solution of hydrofluoric acid (HF) and nitric acid (HNO_3) in distilled water by applying a weak positive voltage of 1–1.5 V to the wire. After one or more minutes of etching, the wire broke at a constriction, leaving a sharp tip within the tube formed by the protruding insulation of the wire. The etched end of the wire was again heated until the insulation softened and contracted around the tip of the wire. Deinsulated tips with diameters of 10–15 μm and a length of about 20 μm could be produced. The impedance of the microelectrodes measured in 0.9% NaCl ranged from 300 kΩ to 1 MΩ (1000 Hz, a/c).

A microelectrode array was constructed by attaching several microelectrodes to the sockets of an Amphenol IC socket connector. To ensure equal distances between individual electrodes, they were held in place by two electron microscope object holder grids (Krüger and Bach, 1981). In addition, two 2 cm long tungsten wires with tapered tips that later served as indifferent electrodes were connected. To stabilize the array, the space between the electrodes was filled with dental acrylic. To record units with different characteristic frequencies (CFs) in the dorsoventral frequency gradient of the tonotopically organized field L (Müller and Leppelsack, 1985; Rübsamen and Dörrscheidt, 1986), the microelectrodes were arranged with different lengths from 2.5 to 4 mm. Microelectrodes were sterilized in ethanol prior to implantation.

2.2. Implantation

Experiments were performed on nine wild-caught adult starlings, *Sturnus vulgaris*, of both sexes that weighed between 70 and 99 g. The care and treatment of these birds were in accordance with the procedures of animal experimentation approved by the Government of Upper Bavaria, Germany. All procedures were performed in compliance with the Guide for the Care and Use of Laboratory Animals.

The birds were given atropine (0.05 ml) subcutaneously to reduce salivation and anesthetized with 0.8–3% halothane. After loss of reflexes, the animals were fixed in an stereotaxic holder by ear bars, with the bill inclined about 45° below the horizontal plane. The body temperature was maintained by means of an electric blanket. Using the caudal bifurcation of the sinus sagittalis as a reference, a small hole was made in the skull 1.5–2.5 mm rostral and 0.8–1.1 mm lateral to the bifurcation, and the overlying dura was incised and reflected. Stereotaxic coordinates were chosen to reach the input layer of field L, L2a. Electrodes were inserted 2.5–4 mm deep into the auditory neostriatum as bundles glued together with saccharose. In seven birds, the electrodes were implanted into the left hemisphere; in a further two animals they were inserted into the right hemisphere. After implantation of the two indifferent electrodes about 7 mm rostral to the sinus bifurcation, the whole array was fixed to the skull with dental cement and the wound was closed using tissue glue. In addition, a socket for the transmitter was glued onto the

electrode array. After the birds awoke from anesthesia, they were carried to their home cages. Recordings started after two or more days but not before the animals had eaten.

2.3. Recordings

To test how many of the electrodes could be used to record auditory-evoked activity, the bird was briefly restrained by wrapping it in a small jacket to prevent wing and leg movements. Pure tones ranging from 200 Hz to 9000 Hz were presented at 70 dB SPL in 100 Hz steps. Electrodes were sequentially connected to a high-impedance amplifier. Recording sites showing sound-elicited activity were noted and investigated in the following experiments with the unrestrained animal.

All multiple-unit data presented here were recorded via radiotelemetry from freely moving birds. During the recording sessions, the bird usually rested calmly on the only perch supplied in a cage (25 cm × 53 cm × 35 cm) inside a custom-built sound-proof booth. They were well habituated to the acoustic stimulation. Food and water were provided ad libitum. An FM radiotransmitter (type 40-71-1, Frederick Haer and Co., USA) with a high-impedance input stage was attached to the socket. Including the battery, the transmitter weighed 5.3 g. The transmitter output was received by a dipole antenna and fed to a commercial FM tuner (Pioneer TX-970), where the signal was demodulated. After filtering (bandpass 500–5000 Hz, high-pass cutoff 48 dB/octave, low-pass cutoff 24 dB/octave) and amplification, the signal was monitored on an oscilloscope and audiomonitor. Optimal tuning of the receiving system to the carrier frequency of the FM transmitter was checked continuously during the recording sessions. The recorded signal was digitized with a 16-bit analog-to-digital converter at a sampling rate of 32 kHz and stored on the disk of a SiliconGraphics Indy Workstation. A software level window discriminator set a threshold level above the highest amplitude of neuronal activity that was used to reject recordings in blocks of 1000 ms whenever such a block contained an artifact. Recordings were interrupted and repeated whenever the starling flew. The software time and level window discriminator separated the neuronal activity ('impulses') from the background activity. Recording sites with a signal-to-noise ratio similar to the one in Fig. 4 were accepted for analysis.

2.4. Stimulus generation

The setup in the sound-proof booth was calibrated with a sound level meter (General Radio 1982 sound level meter) by placing a condenser microphone (General Radio 1/2″ microphone type 1962-9611) at about the location where the bird's head would be in an experiment. The frequency response for pure tones at this location was corrected to vary within ±2 dB.

Tone bursts (duration 250 ms, 10 ms Gaussian rise/fall, inter-stimulus interval 750 ms) and continuous pure tones were produced by a SGI Workstation, using its 16-bit digital-to-analog converter at a sampling rate of 32 kHz. They were adjusted in level by a computer-controlled attenuator (TDT PA 4). Using the workstation's stereo output, the tone burst and continuous tone could be presented simultaneously by mixing the two channels in a Yamaha A-520 hi-fi amplifier. The stimuli were played through a midrange speaker (McFarlow 100MT) mounted at the ceiling of the booth.

To obtain FTCs, responses to 169 (13 frequencies each at 13 sound pressure levels) different frequency-level combinations of 250 ms tone bursts were recorded. The frequency range was centered around the audiovisually estimated most efficient frequency for the recording site. At each level, the sequence of the 13 frequencies was chosen pseudorandomly. Neighboring frequencies differed by a constant factor (between 0.25 and 0.05 octaves at low and high CFs, respectively). Tone bursts were repeated until five artifact-free recordings were obtained. Presentation began at the lowest level of 10 dB SPL, and levels were increased in steps of 5 dB up to a maximum level of 70 dB SPL.

When studying two-tone interaction, the same 169 frequency-level combinations of tone bursts were presented as were used for the FTC. In addition to the tone bursts, a CF tone was played continuously at 20 dB above the best threshold at the CF. This continuously played CF tone is called 'masker' in analogy to psychophysical masking experiments.

To determine the temporal response type characterizing a cell cluster, 20 repetitions of CF tone bursts (80 ms, 3 ms rise/fall, 920 ms inter-stimulus interval) at a level of 70 dB SPL were presented.

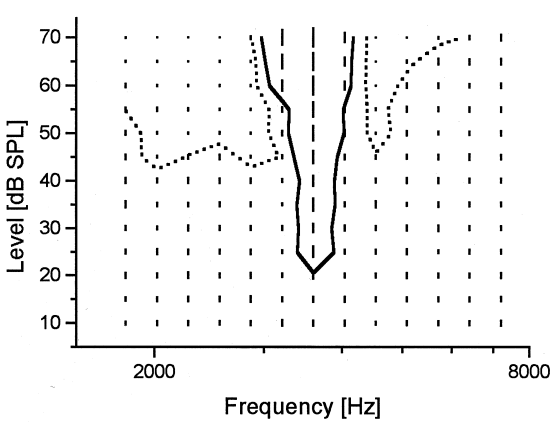

Fig. 1. Example of a response matrix defining the tuning characteristics. The height of the bars indicates the number of impulses per frequency-level combination. A FTC (solid line) and inhibitory sidebands (dotted lines) are added according to the threshold criteria described in the text.

2.5. Data analysis

A FTC was constructed for each recording site from the responses to the 169 different frequency-level combinations (Fig. 1). The tuning curve was calculated from the response to five stimulus repetitions using a statistical threshold criterion derived from signal detection theory. The mean and standard deviation of the spontaneous rate were determined from the number of impulses in 100 ms intervals preceding the presentation of the tone burst for all frequency-level combinations. First, the spontaneous activity recorded in the 100 ms intervals during five repetitions of each frequency-level combination was added up and the mean impulse rate per second was computed. Subsequently, we used the sample of 169 values (13 frequencies presented at 13 levels comprising the matrix of frequency-level combinations) to derive the mean and the standard deviation of the spontaneous impulse rate for each recording site. At the majority of the recording sites (87%), the distribution of the spontaneous impulse rates did not differ significantly from a normal distribution (Kolmogoroff-Smirnov test, $P > 0.05$). The mean and standard deviation of the background activity during the continuous CF tone presentation were calculated in the same manner.

The response threshold was defined as an increase of the mean response rate during presentation of the 250 ms signal by 1.8 standard deviations above the mean spontaneous rate. The threshold for inhibition was a decrease of the mean response rate during signal presentation by 1.8 standard deviations below the mean spontaneous rate. From these FTCs, several response parameters were measured (see Table 1). The threshold criterion of 1.8 standard deviations difference from the mean was applied to make the analysis comparable to that in psychophysical experiments with starlings using a d' of 1.8 as the threshold criterion (e.g., see Langemann et al., 1995).

Table 1
Response parameters measured from FTCs

Parameter	Definition
Characteristic frequency (CF) (Hz)	Stimulus frequency that elicited a neuronal response at a minimal stimulus level
Best threshold (dB SPL)	Response threshold at the CF
Q_{10dB}	CF divided by the bandwidth of a FTC 10 dB above the best threshold
Q_{40dB}	CF divided by the bandwidth of a FTC 40 dB above the best threshold
Bandwidth 70 dB SPL (Hz)	Bandwidth of the FTC at 70 dB SPL
Slope (dB/octave)	Slope at the low-frequency side and the high-frequency side of the FTC (measured between 3 and 23 dB above the best threshold)
Inter-inhibition bandwidth (IIB) (Hz)	Bandwidth between the inhibitory sidebands flanking the FTC at 70 dB SPL

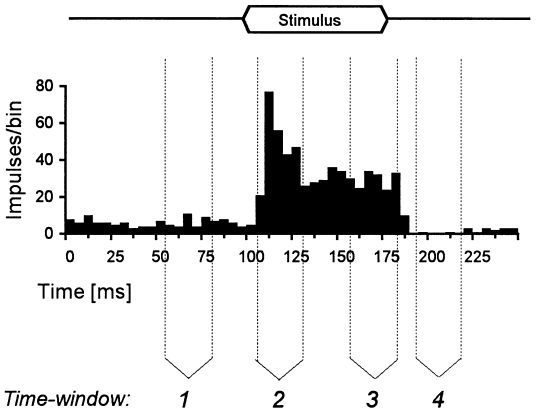

Fig. 2. Stimulus envelope and the corresponding neuronal response at a recording site. The 25 ms time windows used for defining the response type of each cell cluster are indicated by vertical dotted lines. For statistical classification, a 80 ms CF tone was repeated 20 times. Time window 2 started at response onset ('phasic time window'); window 3: response onset+50 ms ('tonic time window'); window 4: response onset+80 ms; window 1: response onset−50 ms. The bin width was 5 ms. The cell cluster shown was classified 'phasic-tonic with OFF inhibition'.

FTCs obtained without a continuously presented CF tone as a background will be called 'FTCs in quiet'. FTCs calculated during two-tone stimulation will be named 'FTCs in CF background'.

The response latency was defined as the time of occurrence of the first of two consecutive 1 ms time bins in the PSTH containing a number of impulses that was at least two standard deviations greater than the mean spontaneous rate. The response type was derived by comparing the number of impulses occurring in four different 25 ms time windows (Fig. 2) using a binomial test. Each of the four time windows was shifted by the response latency. Response types were defined according to the following comparison of time windows. ON activity: phasic: $2 > 3$ and $3 = 1$; tonic: $2 = 3$ and $3 > 1$; phasic-tonic: $2 > 3$ and $3 > 1$. OFF activity: inhibition: $4 < 1$; spontaneous activity: $4 = 1$; excitation: $4 > 1$.

Unless stated otherwise, nonparametric statistics were used. To determine correlations, Spearman's rank correlation coefficient (r_s) was applied. A Wilcoxon test was employed for comparisons on pairs of measurements from the same recording site. All P values are two-tailed.

2.6. Histological verification of electrode penetration

Five to six days before killing the bird, lesions were made at several recording sites by 25 repetitions of pulsed currents (duration 400 ms, 5 μA). An example of a lesioned recording site is shown in Fig. 3. Animals were killed with an overdose of sodium pentobarbital, and, following an initial flush of the circulating system

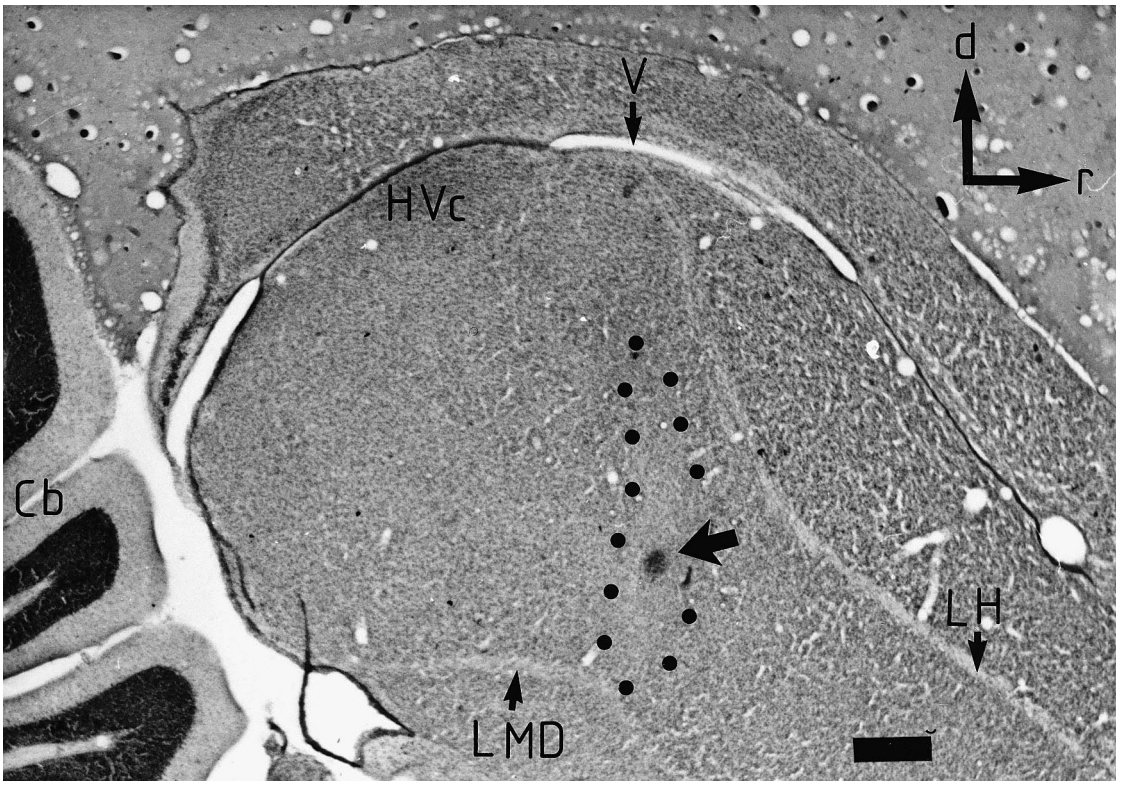

Fig. 3. Photomicrograph of a parasagittal cresyl violet-stained section of the caudal part of a starling's telencephalon. Black dots surround the thalamo-recipient zone L2a of field L. The arrow in L2a indicates a lesion at a recording site. The scale bar is 500 μm. Cb = cerebellum, LH = lamina hyperstriatica, HVc = hyperstriatum ventrale pars caudale, LMD = lamina medullaris dorsalis, V = ventricle.

with a solution containing 0.9% NaCl and 0.5% $NaNO_2$, the brains were fixed by transcardial perfusion of 200 ml paraformaldehyde (6%). The skull and the electrodes were removed and the brain was kept in the fixative for several days. Prior to sectioning, the brain was kept in the same fixative with an additional 10% and 30% sucrose, serving as cryoprotective. After embedding in egg yolk fixed with glutaraldehyde, frozen sagittal sections (50 μm) were cut and counterstained with cresyl violet. Electrode penetrations could be identified because of prominent cells (probably glia) surrounding the electrode trunk.

3. Results

In the present article, we present data from 35 recording sites that were found exclusively to lie within the thalamo-recipient, ventromedial zone of L2, L2a (Karten, 1968; Saini and Leppelsack, 1981; Fortune and Margoliash, 1992; Wild et al., 1993) in the so-called caudal neostriatum (Fig. 3). The response pattern was a phasic-tonic excitation, i.e., a 'primary-like' response. For this type, the discharge rate during the first 25 ms after stimulus onset was significantly higher than the subsequent sustained excitation. Twenty-one of these multiple-unit recordings showed an OFF inhibition, whereas 13 exhibited spontaneous activity after stimulus offset. In one of the 35 clusters, the discharge rate remained at an approximately constant level above spontaneous rate during the ongoing stimulus ('purely tonic'). On average, response latencies to CF tone bursts measured at 70 dB SPL were 9.4 ms (Fig. 5). The latency decreased with increasing CF ($r_s = -0.47$, $P = 0.005$, $n = 35$).

All neuronal responses analyzed in this article were recorded from freely moving birds using chronically implanted microelectrodes and transmitted via an FM

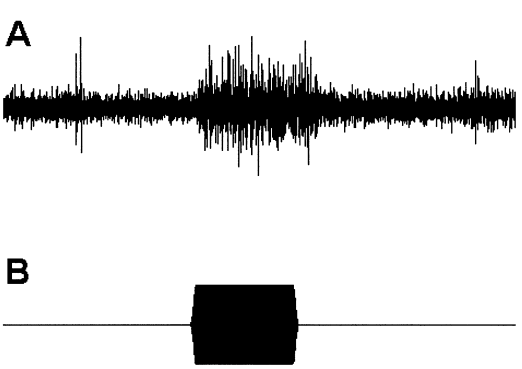

Fig. 4. Multiple-unit activity telemetrically transmitted from a freely moving starling. A: Recording trace of 1 s. B: Envelope of the temporally correlated pure tone stimulus (200 ms duration).

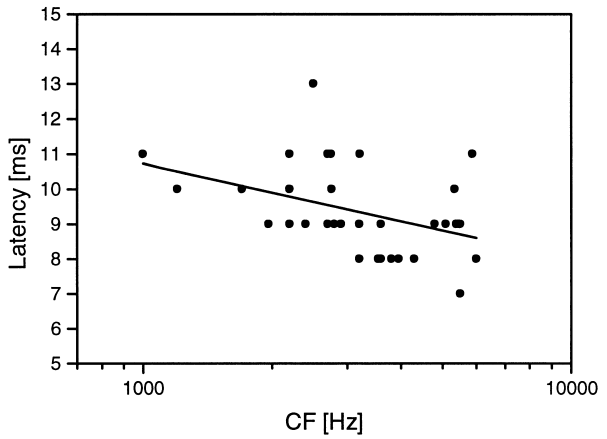

Fig. 5. Latency of all recording sites in L2a plotted against the CF. The latency decreases significantly with increasing CF.

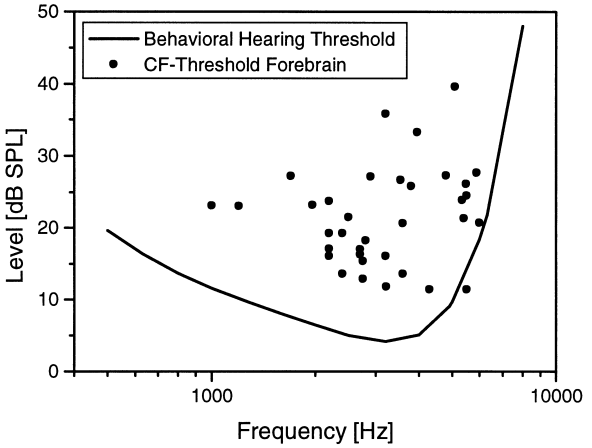

Fig. 6. The thresholds determined from the cell clusters in relation to the characteristic frequency of the recording site. The line shows the starling's behavioral threshold curve obtained from four individuals for comparison (data on absolute threshold with kind permission from U. Langemann).

transmitter attached to the starling's skull. Fig. 4 shows an example of a radiotelemetrically transmitted cluster activity.

3.1. Frequency tuning with single tones

Most of the 35 multi-unit tuning curves showed a simple 'V' shape with no pronounced asymmetries. FTCs with two distinct tips were found in three multi-unit recordings. CFs ranged from 1000 Hz to 5998 Hz, with a minimal best threshold of 11 dB SPL at 4300 Hz and 5505 Hz (Fig. 6). Shifts of the CF could be observed during the first 5 days after electrode implantation at many recording sites. In most cases, the CF shifted to higher frequencies, which may be due to movements of microelectrodes deeper into the tissue. Subsequently, the CF remained stable up to several weeks; changes of frequency tuning were never observed within periods of three or four consecutive days. The longest period between two measurements at the same recording site was 72 days; over this period, the CF remained unchanged and the best threshold varied only by 1 dB. In some cases, the CF at a recording site changed over several weeks. Whenever the change of CF was more than 200 Hz, the recordings were treated as independent data points. There was no correlation between the day of recording after electrode implantation and the best threshold of the recording site ($r_s = 0.0594$, $P = 0.723$, $n = 35$). This indicates a continuously good recording quality of the electrodes. Since a mean impulse rate of 17 spikes/s was observed in a sample of predominantly phasic-tonic or tonic neurons in the starling's auditory forebrain (e.g. Buchfellner, 1987), the mean background activity of 72 impulses/s (±34 impulses/s, S.D.) calculated for all recording sites in the quiet background condition indicates that the multi-unit clusters on average may have consisted of about five cells. However, activity of single units can reach 100 impulses/s in the area of the forebrain from which we recorded in this study (e.g., see Rübsamen and Dörrscheidt, 1986).

Several parameters were used to describe the bandpass filter function of the FTCs (an overview of all statistical values is given in Table 2). Q_{40dB}, but not Q_{10dB}, grew significantly with increasing CF. The absolute bandwidth of the FTC at 10 dB above threshold and 40 dB above threshold, however, grew significantly

Table 2
Mean values of different parameters describing frequency tuning and their correlation with CFs

Parameter	Mean ± S.D.	n	r_s	P
Q_{10dB}	5.2 ± 2.4	35	0.167	0.339
Bandwidth 10 dB above threshold (Hz)	765 ± 402	35	0.566	< 0.001*
Q_{40dB}	3.0 ± 1.2	31	0.377	0.036*
Bandwidth 40 dB above threshold (Hz)	1243 ± 721	31	0.599	< 0.001*
Bandwidth 70 dB SPL (Hz)	1412 ± 563	35	0.507	0.002*
Bandwidth 70 dB SPL (octaves)	0.667 ± 0.283	35	−0.572	< 0.001*
LF slope (dB/octave)	−318 ± 479	35	−0.215	< 0.001*
HF slope (dB/octave)	295 ± 342	35	0.037	0.833
Inter-inhibition bandwidth (Hz)	1585 ± 444	11	0.201	0.553
Inter-inhibition bandwidth (octaves)	0.835 ± 0.312	11	0.279	0.406

*Significant.

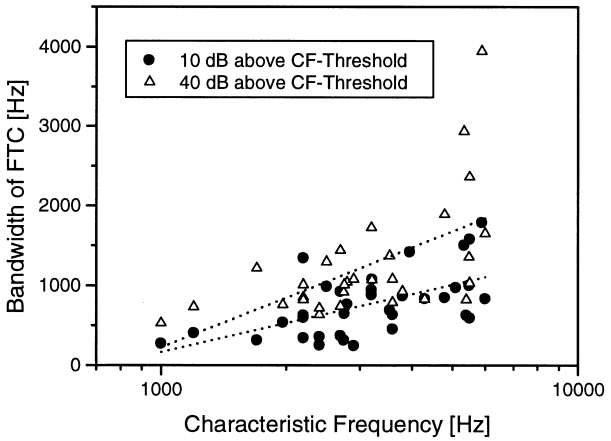

Fig. 7. The tuning curve bandwidths at a tone level of 10 dB and 40 dB above threshold plotted against the CFs of all cell clusters. Both the bandwidths at 10 dB and 40 dB above threshold are significantly correlated with the CF. The dotted lines are the regression lines.

with increasing CF (Fig. 7). At the highest investigated sound pressure level of 70 dB, the excitatory tuning curve bandwidth was also positively correlated with the CF. A second commonly used measure of the filter characteristics are the high- and low-frequency slopes of the flanks of the FTC (Table 2). There was no correlation between either the high- or the low-frequency slope and the CF.

3.2. Inhibitory filter surround

The frequency response at many recording sites in the starling forebrain is not sufficiently characterized by excitation alone. To investigate the inhibitory surround of the excitation area, the reduction of spontaneous activity by tone bursts of a single frequency was quantified. Inhibitory areas were found in more than half of the multi-unit recordings (63%). In 31% of all cell clusters, the FTC was flanked on both sides of the CF by regions in which the response was reduced, thus forming a 'spectral receptive field' with an ON center and OFF surround structure (Fig. 8).

On the low-frequency side, the most sensitive point of the inhibitory area (the tip of the inhibitory sideband) occurred on average at 23.7 dB above threshold at CF, at a spectral distance of 0.579 octaves relative to the CF. Compared to the inhibition on the high-frequency side (mean level: 29.7 dB above threshold, spectral distance: 0.447 octaves), low-frequency inhibition occurred at lower stimulus levels ($P = 0.041$, $n = 11$). The inhibitory sidebands were generally not level independent: frequencies close to the FTC border that reduced the spontaneous activity at low levels were able to excite the recording site at high levels. The mean inter-inhibition bandwidth (IIB), i.e., the bandwidth separating the inhibitory areas at 70 dB SPL, is given in Table 2. At the offset of inhibition, an excitatory rebound was observed in some clusters.

3.3. Frequency tuning during two-tone interaction

For 33 of the 35 recording sites, we measured the responses of cell clusters using a two-tone interaction paradigm. Tone bursts of the same frequency-level combinations as described above were presented simultaneously (i.e., masked) with a continuous pure tone at the CF at a level 20 dB above the FTC threshold. These recordings began about half an hour after the FTC in quiet had been measured.

The continuously presented CF masker increased the mean response rate to 96 impulses/s (±46 impulses/s, S.D.), which is significantly above the mean spontaneous activity of 72 impulses/s (±34 impulses/s, S.D.) determined in the quiet condition ($P = 0.0001$, Wilcoxon test, two-tailed).

The form of the resulting FTC in the presence of a CF background stimulus could be divided into two classes. The first class (19 recording sites) maintained the V-like form and the CF was identical to that of the FTC in quiet. The best threshold, however, shifted towards higher values (Fig. 9A). At the other 14 recording sites, the CF background stimulus influenced the form of the FTC. For example, the cell cluster's tuning curve in Fig. 9B displayed a forked tip during two-tone interaction. Generally, one of the shanks of the split curve was more prominent than the other. Therefore, the CF tips of these units shifted compared to the same recording site in quiet. We observed no systematic direction of the shift – in seven of the 14 recording sites a

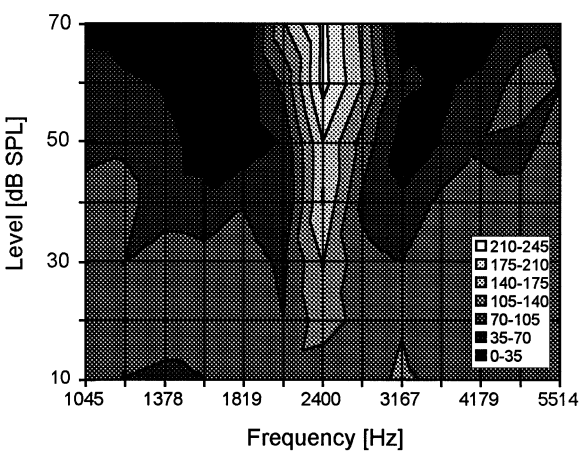

Fig. 8. Some of the phasic-tonic recording sites displayed a receptive field-like structure with spectrum and level as dimensions. Near the CF of this unit (2400 Hz), pure tones elicited increased discharge rates (coded light gray and white). The excitatory region was surrounded by large inhibitory sidebands constricting the FTC (dark gray and black). The legend indicates the number of impulses per second averaged over five repetitions of the stimulus.

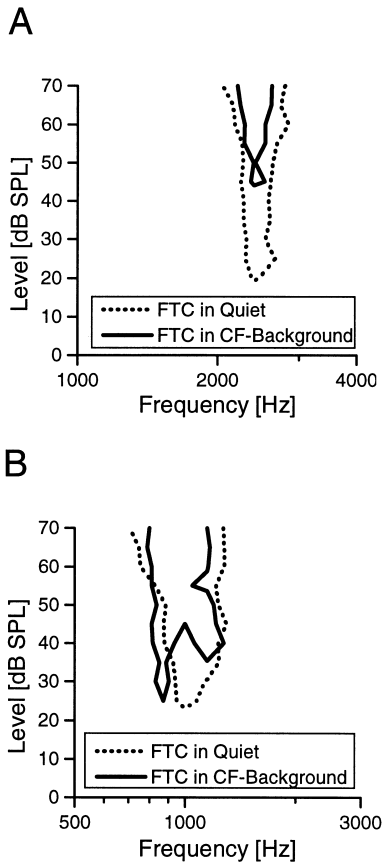

Fig. 9. The form of the FTCs could be divided into two classes when determined using the two-tone paradigm while a continuous CF tone was presented. A: Example of a recording site where the general V shape of the curve in quiet (dotted line) remained in the two-tone interaction paradigm (solid line). B: Example where the tip of the curve in a CF background became forked at the CF.

low-frequency shift occurred and in the other seven sites a high-frequency shift occurred.

Since Q_{10dB} values are strongly dependent on the shape of the tuning curve tip, this parameter was only compared for recording sites that had identical CFs and V-shaped FTCs in both stimulus conditions. The sharpness of the auditory filters grew significantly when the neurons were excited by a continuous CF tone. The mean Q_{10dB} in quiet was doubled during the two-tone interaction paradigm (see Table 3 for statistical values). The mean HF slope of the FTC became significantly steeper during two-tone interaction. At the highest test tone level of 70 dB SPL, the FTC bandwidths decreased on average by 47%. Certain frequencies at the border of the FTC that excited the cells in a silent background did not drive them in the presence of the second tone.

3.4. Influences of CF background on inhibitory surround

The question arose as to whether this observed enhancement of frequency selectivity while stimulating with a CF tone could be correlated with changes in

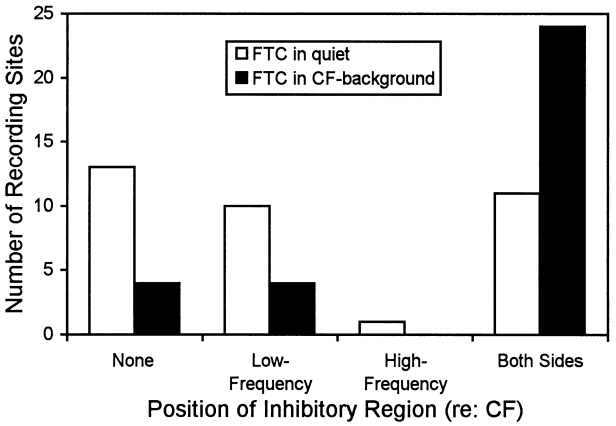

Fig. 10. Compared to the frequency tuning in quiet, units displayed more inhibitory areas during two-tone interaction (righthand pair of columns). The number of recording sites showing inhibitory regions on both sides of the CF was doubled.

the inhibitory sidebands. We tested the hypothesis that increased lateral inhibition could be a mechanism for further sharpening of the FTCs. The CF background had two major effects on the inhibitory sidebands: (1) the overall number of recording sites displaying sideband inhibition grew, and (2) the overall extent of the inhibition was increased.

Since we made recordings using two different stimulus paradigms at identical recording sites, we could directly compare our results for the same cell clusters. Relative to the measurements in quiet, the number of recording sites displaying sideband inhibition on both FTC flanks was more than doubled (73% of all units) through presenting a CF background (Fig. 10).

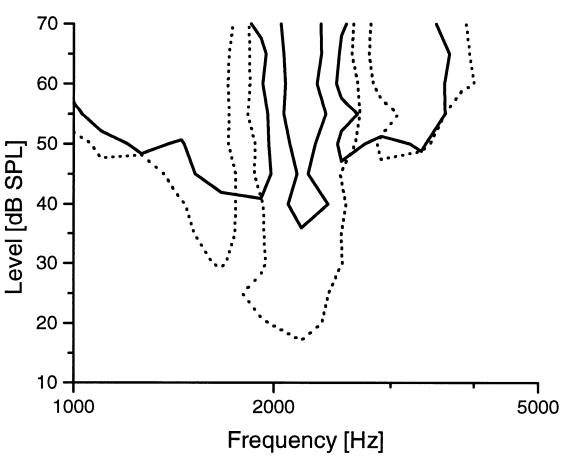

Fig. 11. An example of a recording site for which the FTC changed with the acoustic background. Compared to the FTC and inhibitory sidebands in quiet (dotted line), the FTC of the same cell cluster was sharpened during two-tone interaction (solid line). This was accompanied by an shift of inhibitory sidebands towards the excitatory frequency tuning curve in the two-tone stimulation paradigm. Certain frequencies at the FTC margin that excited the neurons at the recording site in quiet inhibited the neuronal activity in a CF background.

Table 3
Comparison of filter characteristics for FTC in quiet and in CF background

Parameter	FTC in quiet		FTC in CF background		Comparison	
	n	Mean ± S.D.	*n*	Mean ± S.D.	*n*	*P*[a]
Threshold (dB SPL)	35	21.5 ± 6.8	33	40.0 ± 10.2	33	< 0.0001*
Threshold (dB SPL)[b]	21	21.3 ± 7.1	21	44.6 ± 9.2	21	0.0001*
Q_{10dB}[b]	18	5.5 ± 2.1	18	10.3 ± 6.6	18	0.0012*
Bandwidth 10 dB above threshold (Hz)[b]	18	617 ± 226	18	422 ± 250	18	0.0016*
Bandwidth 70 dB SPL (octaves)	35	0.667 ± 0.283	33	0.351 ± 0.221	33	< 0.0001*
LF slope (dB/octave)	35	−319 ± 480	22	−275 ± 305	22	0.884
HF slope (dB/octave)	35	296 ± 342	22	616 ± 621	22	0.026*
Inter-inhibition bandwidth (octaves)	11	0.835 ± 0.312	23	0.727 ± 0.451	11	0.008*

[a]Wilcoxon test, two-tailed. *Significant.
[b]Only recordings where CFs for FTC in quiet and CF background were equal.

The second effect of the CF tone background consisted of a spreading of inhibition over an enlarged frequency range. We analyzed the IIBs of the 11 clusters with two inhibitory sidebands both in quiet and with the CF background and compared them for both background conditions. In these recording sites, the IIB was significantly reduced, on average by 0.11 octaves (see Table 3). In descriptive terms, the inhibitory bands got closer to the CF, seemingly squeezing together the excitatory region and resulting in an enhanced frequency selectivity especially at high levels (Fig. 11). The largest IIB difference observed was 1009 Hz at a CF of 2200 Hz.

In five of 11 cell clusters, the IIB during the masking paradigm was even smaller than the bandwidth of the excitatory tuning curve in quiet determined at the same level. In these cases, the inhibitory sidebands of the tuning curve in the CF background overlapped with the excitatory tuning curve in quiet (see example in Fig. 11). Certain frequencies at the FTC's margin, that excited the cells in quiet, reduced the response while the recording site was driven with a CF tone.

Although the cell clusters were already excited by the continuous masker, inhibition appeared on average on both sides of the excitatory curve at the same levels as in quiet ($P = 0.59$). The frequency distance of the tips of the inhibitory sidebands on the LF side to the CF also remained the same ($P = 0.4$). The tips of the inhibitory sidebands on the HF side, however, shifted towards the CF ($P < 0.01$).

3.5. Temporal aspects of frequency selectivity during masking

To elucidate the mechanisms leading to the observed sharpening of tuning in a CF tone masking background, we studied the time course of inhibition. The first possibility is that the responses reflect non-synaptic suppression effects generated at the level of the basilar papilla. The second possibility is that inhibition, i.e., synaptic interactions providing a restriction of the auditory cell's excitability along the auditory pathway, leads to the observed effect. Since synaptic interactions would require some time – at least some milliseconds – to become established, inhibitory effects should not occur right at stimulus onset. The examples shown in Fig. 12 indicate that the second hypothesis provides a better explanation of the data. Fig. 12A,B shows the spectro-temporal response pattern of the same recording site for a signal presented in quiet or in the presence of a continuous CF tone. In the presence of the background CF tone, the excitatory response area is reduced and frequencies at the border of the excitatory response area in quiet may even reduce the background activity. A more detailed view of the temporal response pattern to tones of five frequencies around the CF is provided in Fig. 12C,D for the unmasked and masked condition, respectively. At the border frequencies of the excitatory response area in quiet (3207 and 4041 Hz), the phasic response is barely affected by the CF background while the tonic response shows a large reduction of activity. This suggests that the mechanism underlying the reduction of activity needs some time to become effective and thus is likely to be inhibition.

To quantify this effect for all recording sites showing sideband inhibition on both sides of the CF, we analyzed frequency tuning in phasic and tonic time windows separately (for details see Fig. 2) and evaluated the Q_{10dB}, the bandwidth of the excitatory FTC at a level of 70 dB SPL and the IIB. All three parameters indicated a highly significant enhancement of frequency selectivity in the tonic response interval. Fifty milliseconds after stimulus onset, the tuning-curves' Q_{10dB} values had, on average, doubled from 3.41 (± 1.97, S.D.) to 7.15 (± 4.49, S.D.) ($P < 0.001$). The tip of the FTC became much sharper with time after stimulus onset. A similar effect could be observed at a level of 70 dB SPL: FTCs defined by the phasic onset response were significantly broader (mean: 0.627 octaves, ± 0.467, S.D.) than defined by the tonic response (mean: 0.346 octaves, ± 0.227, S.D.; $P < 0.0001$). IIBs were also reduced on average from 0.858 octaves (± 0.384, S.D.)

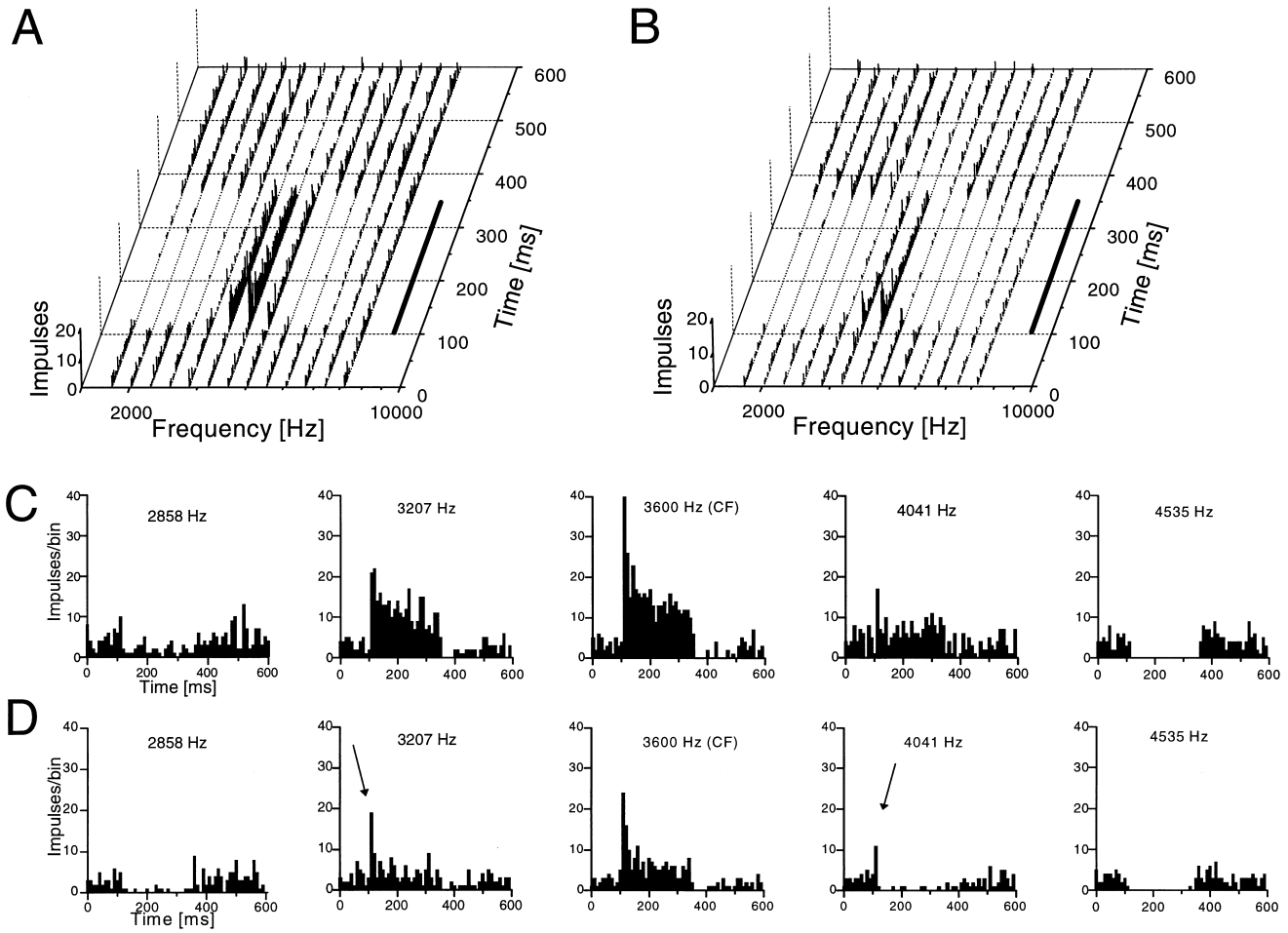

Fig. 12. Peri-stimulus time histograms of one cell cluster under two stimulus conditions. In A and C, single tones were presented in silence; in B and D, the recording site was driven by a continuously presented CF tone. In A and B, data are shown as 3-D plots to elucidate the spectro-temporal dynamics of the responses. For all PSTHs, the 250 ms stimulus (indicated by the bars at the right in A and B) started after 100 ms and was repeated five times at a level of 70 dB SPL; bin width is 5 ms (A and B) and 10 ms (C and D). A: Neuronal response to different frequencies. B: During two-tone interaction, inhibitory areas were increased and frequencies near the CF (which excited the recording site in A) caused a reduction of neuronal activity. C: Temporal course of neuronal activity during stimulation with single tones with frequencies centered around the CF (data taken from A). D: During the masking paradigm, frequencies that excited the cluster vigorously in quiet now elicited only a mild excitation (3207 Hz) or even inhibited the discharge (4041 Hz) (data taken from B). The discharge during the tonic response interval was reduced (at 3207 Hz) or almost eliminated (at 4041 Hz). However, the phasic response still remained (indicated by the arrows).

in the phasic response interval to 0.580 octaves (± 0.242, S.D.) in the tonic response interval ($P < 0.004$). The increase of frequency selectivity measured over the whole stimulus duration during two-tone stimulation can thus mainly be attributed to inhibition starting several milliseconds after response onset.

4. Discussion

We have characterized the spectral tuning properties in the starling's L2a, the input layer of the avian primary auditory forebrain. Compared to FTCs in quiet, auditory filters are significantly sharpened during two-tone stimulation and displayed enhanced frequency selectivity several milliseconds after response onset. These results obtained from freely moving starlings are necessary to explain some of the bird's perceptual abilities in a natural environment and demonstrate the validity of radiotelemetry in studying avian brain functions.

4.1. Response characteristics of recording sites

Temporal and spectral tuning properties are hierarchically organized across different layers of field L (Bonke et al., 1979; Langner et al., 1981; Müller and Leppelsack, 1985; Uno et al., 1991; Lewicki and Arthur, 1996). In the current investigation, we therefore concentrated on the thalamo-recipient zone L2a of the primary auditory forebrain of birds (Karten, 1968; Saini and Leppelsack, 1981; Wild et al., 1993). The phasic-tonic ('primary-like') firing pattern, extensive sideband

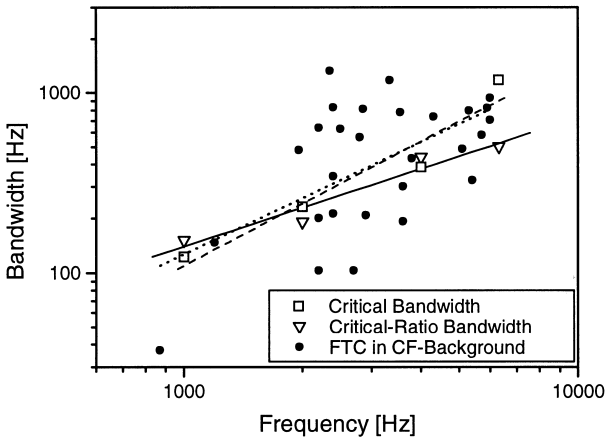

Fig. 13. The FTC bandwidth at 10 dB above threshold during two-tone interaction compared to the psychoacoustically determined mean critical bandwidth and critical ratio of the starling as a function of frequency. The dotted line marks the regression line for the forebrain data; dashed and unbroken lines indicate the critical bandwidth and critical ratio regression lines, respectively (data from Langemann et al., 1995). The starling's critical ratio bandwidth was calculated at a masker spectrum level of 41 dB.

inhibition and short latencies are all characteristic for neurons in the input layer (Leppelsack, 1974; Bonke et al., 1979; Buchfellner et al., 1989; Heil and Scheich, 1991; Leppelsack, 1992, Capsius and Leppelsack, 1996).

Auditory forebrain neurons in the input layer of the starling are rather small in size (average diameter of cell bodies 5–7 μm, Saini and Leppelsack, 1981) and difficult to isolate in a freely moving animal. Since we recorded the activity of cell clusters, we cannot assume a priori that all individual cells in this cluster have identical characteristics. However, because of a well developed tonotopy and a low degree of context sensitivity in L2a (Müller and Leppelsack, 1985; Uno et al., 1991; Lewicki and Arthur, 1996) neighboring neurons can be expected to have very similar or even identical tuning properties. This assumption of a clustered representation of response properties is supported by studies in the mammalian auditory cortex, where single-unit and multi-unit recordings showed good agreement (Shamma et al., 1993; Gaese and Ostwald, 1995). Schreiner and Sutter (1992) reported that single units in different areas of the primary auditory cortical field (AI) were more sharply tuned than multiple units. In the ventral AI (AIv), the larger multiple-unit bandwidth resulted from the scatter of the single units' CFs. If this would also be the case in the starling, we would have underestimated the absolute sharpness of frequency tuning for single units. The observed tuning differences at identical recording sites in the two background conditions (quiet and CF background, respectively), however, would still be valid. Compared to the mammalian auditory cortex, the quality of frequency selectivity in the starling's field L is similar or slightly better (Pelleg-Toiba and Wollberg, 1989; Schreiner and Sutter, 1992; Ehret and Schreiner, 1997).

We found a significant negative correlation ($r_s = -0.47$) between the recording sites' latency and their CFs in field L. This phenomenon may largely be attributed to a delay at low CFs produced in the inner ear, the so-called travel time. Interestingly, Gleich and Narins (1988) calculated a very similar correlation ($r_s = -0.35$, $P < 0.05$) in the starling's cochlear ganglion cells.

4.2. Comparison of frequency selectivity in the starling's periphery and forebrain

Frequency filtering at the auditory periphery has been well studied in the starling (Manley et al., 1985; Manley, 1990). Since many properties describing the tuning of auditory nerve fibers change with characteristic frequency, one can only compare data from similar frequency ranges. The data available from auditory nerve fibers are limited to frequencies below 3.5 kHz. For a comparison with our data from forebrain recordings, we therefore selected original auditory nerve data from a frequency range of 1.7–3.5 kHz from the study of Gleich and Klump (1995) in which a similar set of parameters were measured. The distribution of CFs of both samples were not significantly different ($P = 0.075$, Mann-Whitney U-test). We found no significant increase in the Q_{10dB} values from the periphery to the auditory forebrain units ($P = 0.286$, Mann-Whitney U-test). The Q_{40dB} values, however, grew significantly from 1.80 in the periphery to 2.63 in the forebrain ($P = 0.001$, Mann-Whitney U-test). On average, both HF and LF slopes of the tuning curve flanks were about three times as large in the forebrain (mean HF slope: 332 dB/octave, mean LF slope: −295 dB/octave) compared to the auditory nerve data (mean HF slope: 106 dB/octave, mean LF slope: -99 dB/octave; $P < 0.001$ and $P = 0.003$, respectively, Mann-Whitney U-test). Thus frequency selectivity at low stimulus levels does not differ in auditory nerve fibers and forebrain neurons. However, at high stimulus levels, telencephalic neurons display a significantly increased spectral selectivity.

4.3. Temporal effects of enhanced frequency tuning

Non-synaptic phenomena, like single-tone or two-tone suppression, have already been found in the auditory periphery of the bird's hearing system (Chen et al., 1996; for a review see Manley, 1990). In the bird's cochlea, the latency of suppression does not differ from that of the normal excitatory response (Manley, 1990) and was observed even after the eighth nerve had been cut intracranially, thus abolishing possible feed-

back loops (Temchin, 1988). In the mammalian auditory nerve, latency differences between suppression and excitation at the onset of tone burst ranged from −2 to +2 ms (Arthur et al., 1971). Inhibitory interactions, however, need several milliseconds to become established. The highly significant increase of sideband inhibition in field L when comparing phasic with tonic responses strongly supports the hypothesis of synaptic inhibition. Similarly to our findings concerning frequency tuning, an improved coding of interaural time differences with time after stimulus onset has been reported in the barn owl brainstem (Wagner, 1990).

A putative transmitter suitable for mediating inhibition would be γ-aminobutyric acid (GABA). It is involved in auditory processing on all levels of the avian auditory pathway (Müller, 1988; Müller and Scheich, 1988; Carr et al., 1989) and sharpens tuning curves in the mammalian midbrain (Yang et al., 1992; Vater et al., 1992). GABAergic inhibition has been shown to affect the time course of the neurons' excitatory response, turning tonic responses into phasic-tonic or purely phasic responses (Fujita and Konishi, 1991; LeBeau et al., 1996). The effect observed during two-tone interactions in this study, that the tonic response to frequencies at the FTC border was suppressed while the phasic response interval remained more or less unchanged (see Fig. 12D), may be due to similar mechanisms.

Field L is thought to be the primary source of auditory input to the song nucleus hyperstriatum ventrale pars caudale (Fortune and Margoliash, 1995; Vates et al., 1996). Therefore, the emergence of an enhanced frequency selectivity in L2a over time may have an influence on high-order neurons that respond specifically to songs. A dynamic change of the spectral filter characteristics of neurons over time may be one possible mechanism among others that contributes to the high stimulus selectivity in postsynaptic neurons of L1 and L3, and ultimately even in nuclei of the song system (Margoliash, 1983; Doupe, 1997).

4.4. Spectral filtering and perception of signals in noise

On a perceptual level, the frequency selectivity of an internal filter can be described by its 'critical bandwidth' (CB). Fletcher (1940) attributed the perceptual spectral filtering to frequency tuning properties of the cochlea. However, although cochlea filters provide the first step in auditory filtering, they do not show the level independence of the bandwidth that would be needed to explain some features of critical band measurements (Ehret and Merzenich, 1985; Ehret, 1988; Ehret and Schreiner, 1997).

Psychoacoustic data on spectral filtering (i.e., critical bands and the critical masking ratio) can be directly compared to neural filters in the forebrain. The behavioral critical band measurements, in which a narrowband noise masker centered on the signal is applied simultaneously with the signal, represent a stimulus situation that is comparable to that used in our masking experiments. In quiet, the neurons' 10 dB bandwidth was similar to that observed in the starling's auditory periphery and both were about 2.5 times larger than the CB at 1, 2 and 4 kHz (Langemann et al., 1995). Buus et al. (1995) concluded that the 4 dB bandwidth of peripheral auditory neurons (corresponding to the equivalent rectangular bandwidth of the FTC) has a similar size as a critical band. During the simultaneous masking paradigm, the 10 dB bandwidth of the forebrain neuronal filter functions was significantly reduced to average values that came closer to the psychoacoustically determined auditory filter bandwidth (Fig. 13). This indicates that some of the forebrain clusters may exhibit filter bandwidths that are well below the CB (for a similar observation in the cortical field AI of the anesthetized cat see Ehret and Schreiner, 1997). In addition, the slopes of the high-frequency flank of the FTCs grew significantly, indicating that the flanks of the neuronal filter functions became very steep. This sharpening of the neuronal filters made their bandwidth more independent of the level which is typical for behavioral critical ratio data (the starling's critical ratio bandwidth is similar to its critical bandwidth). This level independence has also been shown in the central nucleus of the anesthetized cat inferior colliculus (ICc) by Ehret and Merzenich (1985, 1988). They found that critical band estimates from the cat's ICc neurons match results from behavioral measurements with the same stimulus paradigm. A similar correlation has been observed in parts of the cat cortical area AI (Ehret and Schreiner, 1997).

The observation that the neural filter functions of cell clusters in the starling forebrain become more sharply tuned over time bears on the issue of perceptual changes in the frequency selectivity of the auditory system with ongoing time of a stimulus. Several psychophysical studies in humans have indicated that the perceptual CB may develop over time being broader for short-duration signals than for long-duration signals (for a recent review of the psychoacoustic evidence see Hant et al., 1997). Hant et al. (1997) suggested that these changes in the bandwidth of auditory filters reflect the action of higher-level neural processing of the output from the cochlea that may require time to develop. In the starling, we have shown that a narrowing of the neural filters occurs over ongoing time of the stimulus. It would be interesting to determine the time course describing the change in the starling's perceptual bandwidth psychophysically and compare it to the time course of the change in the bandwidth of neurons in this bird's auditory forebrain.

4.5. Radiotelemetry of unit activity in a songbird: its scope and limits

In recent years, there has been a growing interest in correlating an animal's behavior with its neuronal activity. Although several interesting papers have dealt with the method of telemetry in brain research (Skutt et al., 1967; Eichenbaum et al., 1977; Pinkwart and Borchers, 1987), there are few detailed studies using radio transmitters to record unit activity (e.g., Goldberg and Moulton, 1987; Scharmann, 1996).

Using a light-weight FM transmitter with a high-impedance input stage, we succeeded in studying auditory evoked, multiple-unit activity in the forebrain of the starling, a small bird species. No differences in the signal-to-noise ratio of multi-unit impulses directly fed into an amplifier (a method that we used to test the quality of the microelectrodes immediately after their implantation) and telemetrically transmitted potentials were observed. Cluster activity could be recorded up to several weeks or even months from individual electrodes, and the response characteristics were stable at least over a time period of several days. This allowed a detailed study of the neural response patterns, which are more difficult to obtain in acute experiments. Furthermore, artifacts caused by anesthesia, as recently described in the starling forebrain (Capsius and Leppelsack, 1996), were excluded. An important advantage of telemetric recording was the reduced stress to the birds: they were able to move and fly freely during the recording session and had access to food and water; handling of the animals was only necessary when mounting the transmitter or when switching to another electrode.

Some problems appeared using radiotelemetric transmission of unit activity. Recording artifacts occurred whenever the birds made large movements or flew. By implementing the artifact rejection described in Section 2, we obtained artifact-free recordings. During recording, care had to be taken for optimal tuning of the receiving system to the carrier frequency of the FM transmitter. Sub-optimal tuning resulted in a reduced amplitude of the signal. Tuning was constantly controlled and corrected when necessary.

In general, radiotelemetry is an elegant tool for studying neuronal activity in the brain of awake animals. The study of brain functions in birds performing a behavioral task (Scharmann, 1996) may benefit greatly from this technique.

Acknowledgments

We thank Michael G. Scharmann for valuable support during the experiments. Dirk Kautz, Christine Köppl, Hans-Joachim Leppelsack, Geoffrey A. Manley and Hermann Wagner provided critical and helpful comments on a previous version of the manuscript. We thank Søren Buus and two anonymous reviewers who helped to improve the manuscript. The study was supported by a grant to G.M.K. from the DFG within the SFB 204 'Gehör'.

References

Arthur, R.M., Pfeiffer, R.R., Suga, N., 1971. Properties of 'two-tone inhibition' in primary auditory neurons. J. Physiol. 212, 593–609.

Bonke, D., Scheich, H., Langner, G., 1979. Responsiveness of units in the auditory neostriatum of the guinea fowl (*Numida meleagris*) to species-specific calls and synthetic stimuli. I. Tonotopy and functional zones of field L. J. Comp. Physiol. A 132, 243–255.

Buchfellner, E., 1987. Untersuchungen zur Kodierung von Pausen in weißem Rauschen durch Neurone des caudalen Telencephalon des Staren (*Sturnus vulgaris*). Diplom Thesis, Technische Universität, Munich.

Buchfellner, E., Leppelsack, H.-J., Klump, G.M., Häusler, U., 1989. Gap detection in the starling (*Sturnus vulgaris*). II. Coding of gaps by forebrain neurons. J. Comp. Physiol. A 164, 539–549.

Buus, S., Klump, G.M., Gleich, O., Langemann, U., 1995. An excitation-pattern model for the starling (*Sturnus vulgaris*). J. Acoust. Soc. Am. 98, 112–124.

Capsius, B., Leppelsack, H.-J., 1996. Influence of urethane anesthesia on neural processing in the auditory cortex analogue of a songbird. Hear. Res. 96, 59–70.

Carr, C.E., Fujita, I., Konishi, M., 1989. Distribution of GABAergic neurons and terminals in the auditory system of the barn owl. J. Comp. Neurol. 286, 190–207.

Chen, L., Salvi, R.J., Trautwein, P.G., Powers, N., 1996. Two-tone rate suppression boundaries of cochlear ganglion neurons in normal chickens. J. Acoust. Soc. Am. 100, 442–450.

Doupe, A.J., 1997. Song- and order-selective neurons in the songbird anterior forebrain and their emergence during vocal development. J. Neurosci. 17, 1147–1167.

Ehret, G., 1988. Frequency resolution, spectral filtering, and integration on the neuronal level. In: Edelman, G.M., Gall, W.E., Cowan, W.M. (Eds.), Auditory Function: Neurobiological Basis of Hearing, Wiley, New York, pp. 363–384.

Ehret, G., 1995. Auditory frequency resolution in mammals: from neuronal representation to perception. In: Manley, G.A., Klump, G.M., Köppl, C., Fastl, H., Oeckinghaus, H. (Eds.), Advances in Hearing Research. Proceedings of the 10th International Symposium on Hearing, World Scientific, Singapore, pp. 387–397.

Ehret, G., Merzenich, M.M., 1985. Auditory midbrain responses parallel spectral integration phenomena. Science 227, 1245–1247.

Ehret, G., Merzenich, M.M., 1988. Complex sound analysis (frequency resolution, filtering and spectral integration) by single units of the interior colliculus of the cat. Brain Res. Rev. 13, 139–163.

Ehret, G., Schreiner, C.E., 1997. Frequency resolution and spectral integration (critical band analysis) in single units of the cat primary auditory cortex. J. Comp. Physiol. A 181, 635–650.

Eichenbaum, H., Pettijohn, D., Deluca, A.M., Chorover, S.L., 1977. Compact miniature microelectrode-telemetry system. Physiol. Behav. 18, 1175–1178.

Evans, E.F., Pratt, S.R., Spenner, H., Cooper, N.P., 1992. Comparisons of physiological and behavioural properties: auditory frequency selectivity. In: Cazals, Y., Horner, K., Demany, L. (Eds.), Auditory Physiology and Perception, Pergamon Press, Oxford, pp. 159–169.

Fletcher, H., 1940. Auditory patterns. Rev. Mod. Physiol. 12, 47–65.

Fortune, E.S., Margoliash, D., 1992. Cytoarchitectonic organization and morphology of cells of the field L complex in male zebra finches (*Taeniopygia guttata*). J. Comp. Neurol. 325, 388–404.

Fortune, E.S., Margoliash, D., 1995. Parallel pathways and convergence onto HVc and adjacent neostriatum of adult zebra finches (*Taeniopygia guttata*). J. Comp. Neurol. 360, 413–441.

Fujita, I., Konishi, M., 1991. The role of GABAergic inhibition in processing of interaural time difference in the owl's auditory system. J. Neurosci. 11, 722–739.

Gaese, B.H., Ostwald, J., 1995. Temporal coding of amplitude and frequency modulation in the rat auditory cortex. Eur. J. Neurosci. 7, 438–450.

Gleich, O., Klump, G.M., 1995. Temporal modulation transfer functions in the European starling (*Sturnus vulgaris*): II. Responses of auditory-nerve fibres. Hear. Res. 82, 81–92.

Gleich, O., Narins, P.M., 1988. The phase response of primary auditory afferents in a songbird (*Sturnus vulgaris* L.). Hear. Res. 32, 81–92.

Goldberg, S.J., Moulton, D.G., 1987. Olfactory bulb responses telemetered during an odor discrimination task in rats. Exp. Neurol. 96, 430–442.

Hant, J.J., Strope, B.P., Alwan, A.A., 1997. A psychoacoustic model for the noise masking of plosive bursts. J. Acoust. Soc. Am. 101, 2789–2802.

Heil, P., Scheich, H., 1991. Functional organization of the avian auditory cortex analogue. II. Topographic distribution of latency. Brain Res. 39, 121–125.

Jacob, R., Krüger, J., 1991. Manufacture of sharpened microelectrodes from varnished wire. J. Neurosci. Methods 38, 89–93.

Karten, H.J., 1968. The ascending auditory pathway in the pigeon (*Columba livia*). II. Telencephalic projections of the nucleus ovoidalis thalami. Brain Res. 11, 134–153.

Katsuki, Y., Sumi, T., Uchiyama, H., Watanabe, T., 1958. Electric responses of auditory neurons in cat to sound stimulation. J. Neurophysiol. 21, 469–588.

Klump, G.M., 1996. Bird communication in the noisy world. In: Kroodsma, D.E., Miller, E.H. (Eds.), Ecology and Evolution of Acoustic Communication in Birds. Cornell University Press, Ithaca, NY, pp. 321–338.

Klump, G.M., Langemann, U., 1995. Comodulation masking release in a songbird. Hear. Res. 87, 157–164.

Krüger, J., Bach, M., 1981. Simultaneous recording with 30 microelectrodes in monkey visual cortex. Exp. Brain Res. 41, 191–194.

Langemann, U., Klump, G.M., Dooling, R.J., 1995. Critical bands and critical ratio bandwidth in the European starling. Hear. Res. 84, 167–176.

Langner, G., Bonke, D., Scheich, H., 1981. Neuronal discrimination of natural and synthetic vowels in field L of trained mynah birds. Exp. Brain Res. 43, 11–24.

LeBeau, F.E.N., Rees, A., Malmierca, M.S., 1996. Contribution of GABA- and glycine-mediated inhibition to the monaural temporal response properties of neurons in the inferior colliculus. J. Neurophysiol. 75, 902–919.

Leppelsack, E.H., 1992. Eine Kartierung auditorischer Antwortareale im caudalen Vorderhirn des Staren (*Sturnus vulgaris*) unter Verwendung von Reintönen, arteigenen Lauten und deren akustischen Modellen. Doctoral Thesis, Technische Universität, Munich.

Leppelsack, H.-J., 1974. Funktionelle Eigenschaften der Hörbahn im Feld L des Neostriatum caudale des Staren (*Sturnus vulgaris* L., Aves). J. Comp. Physiol. 88, 271–320.

Lewicki, M.S., Arthur, B.J., 1996. Hierarchical organization of auditory temporal context sensitivity. J. Neurosci. 16, 6987–6998.

Manley, G.A., 1990. Peripheral Hearing Mechanisms in Reptiles and Birds, Springer, Berlin.

Manley, G.A., Gleich, O., Leppelsack, H.-J., Oeckinghaus, H., 1985. Activity patterns of cochlear ganglion neurons in the starling. J. Comp. Physiol. A 157, 161–181.

Margoliash, D., 1983. Acoustic parameters underlying the responses of song-specific neurons in the white-crowned sparrow. J. Neurosci. 3, 1039–1057.

Müller, C.M., 1988. Distribution of GABAergic perikarya and terminals in the centers of the higher auditory pathway of the chicken. Cell Tissue Res. 252, 99–106.

Müller, C.M., Leppelsack, H.-J., 1985. Feature extraction and tonotopic organization in the avian auditory forebrain. Exp. Brain Res. 59, 587–599.

Müller, C.M., Scheich, H., 1988. Contribution of GABAergic inhibition to the response characteristics of auditory units in the avian forebrain. J. Neurophysiol. 59, 1673–1689.

Pelleg-Toiba, R., Wollberg, Z., 1989. Tuning properties of auditory cortex cells in the awake squirrel monkey. Exp. Brain Res. 74, 353–364.

Pickles, J.O., 1979. Psychophysical frequency resolution in the cat as determined by simultaneous masking and its relation to auditory-nerve resolution. J. Acoust. Soc. Am. 66, 1725–1732.

Pinkwart, C., Borchers, H.-W., 1987. Miniature three-function transmitting system for single neuron recording, wireless brain stimulation and marking. J. Neurosci. Methods 20, 341–352.

Rübsamen, R., Dörrscheidt, G.J., 1986. Tonotopic organization of the auditory forebrain in a songbird, the European starling. J. Comp. Physiol. A 158, 639–646.

Saini, K.D., Leppelsack, H.-J., 1981. Cell types of the auditory caudomedial neostriatum of the starling (*Sturnus vulgaris*). J. Comp. Neurol. 198, 209–229.

Scharmann, M.G., 1996. Stoffwechselphysiologische und elektrophysiologische Untersuchungen zur Modulation neuronaler Verarbeitung beim Staren (*Sturnus vulgaris* L.), Doctoral Thesis, Technische Universität, Munich.

Schreiner, C.E., Sutter, M.L., 1992. Topography of excitatory bandwidth in cat primary auditory cortex: single-neuron versus multiple-neuron recordings. J. Neurophysiol. 68, 1487–1502.

Shamma, S.A., Fleshman, J.W., Wiser, P.R., Versnel, H., 1993. Organization of response areas in ferret primary auditory cortex. J. Neurophysiol. 69, 367–383.

Skutt, H.R., Beschle, R.G., Moutton, D.G., Koella, W.P., 1967. New subminiature amplifier-transmitter for telemetering biopotentials. Electroenceph. Clin. Neurophysiol. 22, 275–277.

Suga, N., Tsuzuki, K., 1985. Inhibition and level-tolerant frequency tuning in the auditory cortex of the mustached bat. J. Neurophysiol. 53, 1109–1145.

Temchin, A.N., 1988. Unusual discharge patterns of single fibers in the pigeon's auditory nerve. J. Comp. Physiol. A 163, 99–115.

Uno, H., Ohno, Y., Yamada, T., Miyamoto, K., 1991. Neural coding of speech sound in the telencephalic auditory area of the mynah bird. J. Comp. Physiol. A 169, 231–239.

Vater, M., Habbicht, H., Kössl, M., Grothe, B., 1992. The functional role of GABA and glycine in monaural and binaural processing in the inferior colliculus of horseshoe bats. J. Comp. Physiol. A 171, 541–553.

Vates, G.E., Broome, B.M., Mello, C.V., Nottebohm, F., 1996. Auditory pathways of caudal telencephalon and their relation to the song system of adult male zebra finches (*Taeniopygia guttata*). J. Comp. Neurol. 366, 613–642.

Wagner, H., 1990. Receptive fields of neurons in the owl's auditory brainstem change dynamically. Eur. J. Neurosci. 2, 949–959.

Wild, J.M., Karten, H.J., Frost, B.J., 1993. Connections of the auditory forebrain in the pigeon (*Columba livia*). J. Comp. Neurol. 337, 32–62.

Yang, L., Pollak, G.D., Resler, C., 1992. GABAergic circuits sharpen tuning curves and modify response properties in the mustache bat inferior colliculus. J. Neurophysiol. 68, 1760–1774.